IOPscience iopscience.iop.org

Home Search Collections Journals About Contact us My IOPscience

Magnetic satellites in the incommensurate phase of pure and doped $NiBr_2$

This article has been downloaded from IOPscience. Please scroll down to see the full text article.

1989 J. Phys.: Condens. Matter 1 6551

(http://iopscience.iop.org/0953-8984/1/37/004)

View the table of contents for this issue, or go to the journal homepage for more

Download details:
IP Address: 171.66.16.93
The article was downloaded on 10/05/2010 at 18:48

Please note that terms and conditions apply.

J. Phys.: Condens. Matter 1 (1989) 6551–6558. Printed in the UK

Magnetic satellites in the incommensurate phase of pure and doped $NiBr_2$

I H Odisho and H M Al-Dorry
Physics Department, College of Education, Mustansryia University, Baghdad, Iraq

Received 3 June 1988, in final form 14 November 1988

Abstract. $NiBr_2$, pure or Fe-doped, undergoes a phase transition from commensurate to incommensurate structure at $T_{IC} = 22$K. The incommensurate phase (helical magnetic structure) is accompanied by the appearance of a hexagon of satellites around the (003) and $(10\bar{1})$ magnetic reflections, which moves out from the commensurate peak as the temperature is lowered until it is complete at 4.2 K. The propagation vector in pure $NiBr_2$ lies in the basal plane a^*b^* and along the $\langle 110 \rangle$ direction whereas in doped $NiBr_2$ it can lie in almost any direction within the a^*b^* plane. A model that fits intensities distributed around a ring to those of the hexagon of satellites around the (003) magnetic reflection is discussed and used as a basis for calculations.

1. Introduction

$NiBr_2$, with the $CdCl_2$ crystal structure—hexagonal ($R\bar{3}m$), is unique among the metamagnetic transition-metal dihalides, and probably among all magnetic materials, in undergoing a transition from a commensurate collinear magnetic structure to an incommensurate helical spin structure with a propagation length that is a smooth function of temperature (Day and Ziebeck 1979, 1980, Adam *et al* 1980). Above T_{IC} it has a collinear magnetic structure consisting of sheets of ferromagnetically coupled spins lying within the basal plane, successive sheets being coupled antiferromagnetically as in $NiCl_2$. The onset of the incommensurate phase, in which the spins still lie within the basal plane but describe a helix along the $\langle 110 \rangle$ direction with wavevector $\boldsymbol{k}_0 = [0.027, 0.027, \frac{3}{2}]$ at $T = 4.2$ K (figure 1; see also Adam *et al* 1980), is accompanied by the appearance of a hexagon of satellites around the (003) and $(10\bar{1})$ magnetic reflections, which moves out from the commensurate peak as the temperature is lowered (Day and Ziebeck 1980, Day *et al* 1976). In an effort to understand the origin of the helical phase and the driving mechanism of the commensurate–incommensurate transition, Regnault *et al* (1982) measured the spin waves for the $\langle 110 \rangle$ direction at $T = 4.2$ K of $NiBr_2$ in order to determine the exchange and anisotropy parameters, which help to describe the unusual helimagnetic–antiferromagnetic transition that occurs at $T = 22.8$ K.

In $Ni_{0.92}Zn_{0.08}Br_2$, on the other hand, random substitution of Zn ions into the lattice disorders the propagation direction of the helix but leaves the propagation length sufficiently well defined that the satellite structure now consists of a ring in the a^*b^* plane (Day *et al* 1981). This behaviour is relevant to the theoretical work by Rastelli *et al* (1979) showing that the incommensurate phase is stable because of competition

0953-8984/89/376551 + 08 $02.50 © 1989 IOP Publishing Ltd

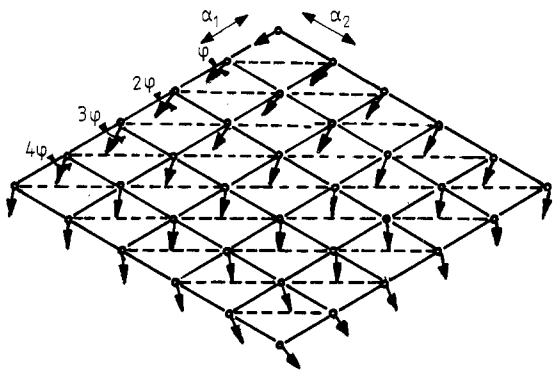

Figure 1. Helimagnetic ordering within the basal plane for $NiBr_2$ at $T = 4.2$ K.

between the near-neighbour ferromagnetic exchange and antiferromagnetic second- and third-near-neighbour exchange, so the magnetic order should be peculiarly susceptible to changes in the lattice occurring on doping with non-magnetic ions.

In view of the observation of the satellite structure in both pure and doped $NiBr_2$, the aim of the present work is to fit a set of intensities measured in reciprocal space to a model in which the major hexagonal satellite distribution is superimposed on a ring of intensity representing a degree of disorder in the propagation direction. It also constitutes a test of the applicability of the multidetector diffractometer D16 to studying incommensurate magnetic structure at low temperature, since it was the first time the multidetector had been used for this purpose. The fitting is also being extended to include the temperature dependence of the (003) magnetic reflection plane (termed $(003)_m$) through the commensurate–incommensurate phase transition at 22 K.

2. Experimental details

Single-crystal samples of pure and Fe-doped nickel dibromide ($NiBr_2$) were grown by the Bridgman–Stockbarger technique. From these, single crystals of approximate dimensions $5 \times 5 \times 1$ mm^3 were cleaved. These were aligned with $\langle 00l \rangle$ and $\langle h00 \rangle$ vectors

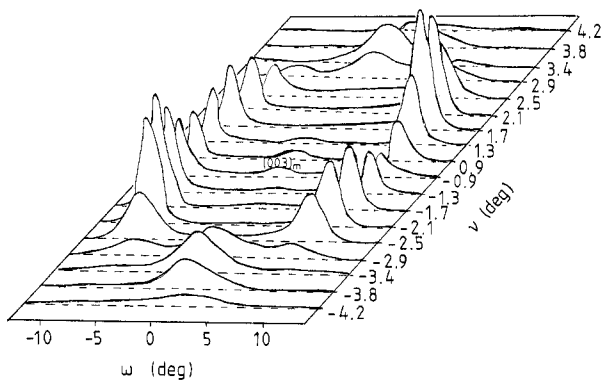

Figure 2. A perspective diagram of a portion of the observed satellite intensity at 4.2 K in ω, ν space around $(003)_m$.

Table 1. Observed positions of satellites in reciprocal space, intensities and propagation lengths and directions φ(WRT a^*) as functions of temperature for $NiBr_2$, around (*a*) $(003)_m$ and (*b*) $(10\bar{1})_m$.

T (K)	2θ (deg)	ω (deg)	ν (deg)	I/I_0 (sat.)	$I/I_0\,(003)_m$	τ (Å^{-1})	φ (deg)
(*a*)							
22	21.35	3.9	0.61	56	100	0.0060	22.7
20	21.35	5.2	0.83	79	11	0.0084	23.3
18	21.35	6.5	0.93	80	8	0.0098	26.2
4.2	21.35	8.4	1.70	100	1	0.0138	28.8
(*b*)							
22	91.84	0.96	0.55	46	100	0.0060	23.9
20	91.84	1.33	0.72	76	15.5	0.0084	26.1
18	91.84	1.74	0.89	83	13.1	0.0098	24.5
4.2	91.84	2.15	1.60	100	12.7	0.0138	27.4

in the horizontal plane and enclosed in a variable-temperature cryostat allowing measurements to be made down to 4.2 K. Diffraction measurements were made on the four-circle diffractometer D16 using a neutron beam of wavelength 4.52 Å and a sample-to-detector separation of 500 mm. The magnetic satellite structures around the (003) and $(10\bar{1})$ magnetic reflections, as the temperature was varied from 22 to 4.2 K, were examined, intensities being collected as functions of 2θ and ν across the 64 × 16 multi-detector grid while the table angle ω was increased in steps. The instrumental resolution defined by the spacing between the elements of the multidetector was 0.29, 0.15, 0.57° in 2θ, ω, ν respectively. This was good enough to enable us to resolve the six individual satellites. The satellites were represented at the multidetector grid by 2θ (64 elements running down), ν (16 elements running across) and ω (the angle in steps of 0.5°).

3. Analysis of results

Figure 2 shows a portion of the data in the form of a perspective diagram of the satellite intensity observed at 4.2 K in ω, ν space around $(003)_m$. The results are consistent with

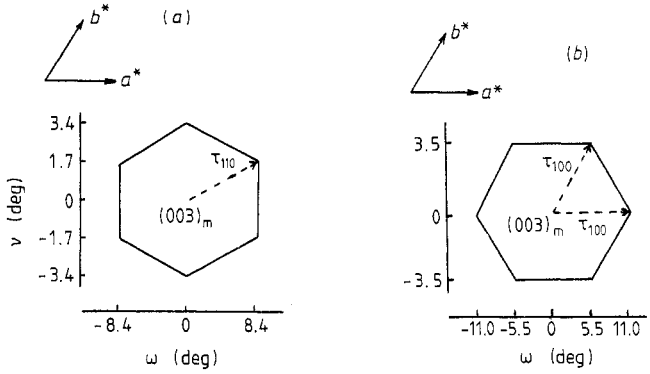

Figure 3. Hexagonal satellites around $(003)_m$ in the a^*b^* plane of the reciprocal lattice at 4.2 K (*a*) for pure $NiBr_2$, (*b*) for $Fe_{0.1}Ni_{0.9}Br_2$. (The intensities of the satellites are given in table 2.)

Table 2. Intensities of hexagonal satellites at 4.2 K as indicated in figure 2. (*a*) $NiBr_2$ (τ = 0.0138 Å^{-1}). (*b*) $Fe_{0.1}Ni_{0.9}Br_2$ (τ = 0.0151 Å^{-1}).

I (10^{-3} counts)		ω	ν
$(003)_m$	$(00\bar{3})_m$	(deg)	(deg)
(*a*)			
18	17	3.4	0.0
59	55	8.4	1.7
22	19	8.4	−1.7
17	16	−3.4	0.0
54	57	−8.4	−1.7
20	18	−8.4	1.7
(*b*)			
17	19	11.0	0.0
10	12	5.5	−3.5
20	14	5.5	−3.5
12	15	−11.0	0.0
12	14	−5.5	3.5
11	8	5.5	3.5

a regular hexagon of satellites in the a^*b^* plane of the reciprocal lattice, characterised by a helical propagation vector as illustrated in figure 3. The procedure for fitting the set of intensities measured in the 2θ, ω, ν space to a model in which the major hexagonal satellite distribution is superimposed on a ring of intensity representing a degree of disorder in the propagation direction is given herein.

A ring simulated by 40 points separated by steps of 9° was chosen. From the geometry of the reciprocal space around the (003) reflection (see Appendix 1), ω and ν (in degrees) were calculated for a given magnitude of the propagation vector, τ (in Å^{-1}). The corresponding values for ω and ν in terms of elements represented at the multidetector were calculated at these points (see Appendix 2).

The value of the peak intensity from the scan of $(003)_m$ at 28 K (commensurate phase) was used to calculate the distribution of intensities at the locations of ω- and ν-elements for the 40 points, this calculation being preceded by a scaling and weighting of the intensities, giving extra weight to the direction ⟨110⟩, to bring the intensities in the calculated pattern to the observed values. Initially the calculation was done by taking only integer values of ω- and ν-elements, neglecting the fractional values. Because of the significant difference between the observed and calculated intensities, the distributions of intensities were then recalculated by interpolating the values of the peak intensities for the fractions corresponding to precise locations of points from the nearest integer values of ω- and ν-elements. The differences between the observed and calculated patterns were obtained after interpolating to the centres of both patterns using the fractions.

4. Discussion

Table 1 shows the satellites for $NiBr_2$ around $(003)_m$ and $(10\bar{1})_m$ as a function of temperature. In the temperature range 22–20 K, the commensurate–incommensurate

phases coexist. This finding agrees with the reported result (Adam *et al* 1980) that in zero field the commensurate and satellite reflections of $NiBr_2$ coexist over about 1 K. At temperatures below 20 K the commensurate phase disappears and the satellite structure grows until it is complete at 4.2 K.

The satellite structure around $(003)_m$, represented in figure 3(*a*) consists of a regular hexagon in the a^*b^* plane with a propagation vector lying along $\langle 110 \rangle$ direction and reaches a limiting value of 0.0138 $Å^{-1}$ at 4.2 K. In doped $NiBr_2$, on the other hand, the introduction of 0.1 mol% Fe has introduced a large disorder in the propagation direction, so instead of lying along the $\langle 110 \rangle$ direction it has almost equal probability of lying in any direction within the a^*b^* plane, e.g. along the $\langle 100 \rangle$ direction (figure 3(*b*)), and its magnitude has increased to 0.0151 $Å^{-1}$ at 4.2 K (see table 2). Such disorder has been found in $NiBr_2$ doped with Zn (Day *et al* 1981) and the reason for the existence of the helical phase is a competition between the near-neighbour ferromagnetic exchange constant J_1 and the antiferromagnetic second- and third-nearest-neighbour exchange

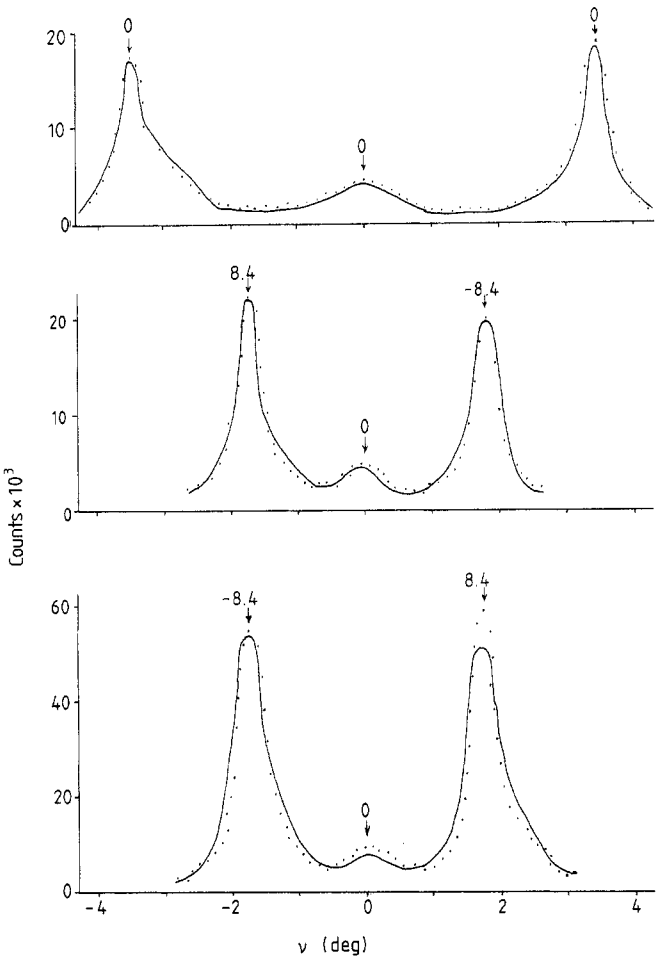

Figure 4. Observed and calculated profiles for $(003)_m$ and satellites for $NiBr_2$ at 4.2 K. The full circles show observed data and the full curves were calculated assuming a smooth ring of intensity centred at $(003)_m$. The arrows give values of ω (in deg).

constants J_2 and J_3. Moreover, the disorder in the propagation vector may result from the random distribution of Fe ions in the lattice, which causes local fluctuation in J_2 and J_3, so varying the propagation direction randomly through the crystal.

Figure 4 shows that the best fit to the experimental profiles was obtained with a uniform distribution of intensity around a ring. A slight improvement in the fit was obtained by giving a small ($\simeq 9\%$) extra weight to the $\langle 110 \rangle$ direction. A similar fitting procedure for the $(10\bar{1})_m$ satellite reflection profiles also gave a good fit when a circular distribution was used. A similar fitting model was extended to include the experimental profiles at 22 K, and figure 5 shows that good agreement between observed and calculated profiles was obtained. It also shows the coexistence of the collinear commensurate phase and the helical incommensurate phase.

Finally, it can be noted that replacing only 10% of the magnetic ions in the $NiBr_2$ lattice by non-magnetic ones has a dramatic effect on the propagation direction, disordering it almost completely, while the propagation length remains well defined and only increases in magnitude by 9.4%.

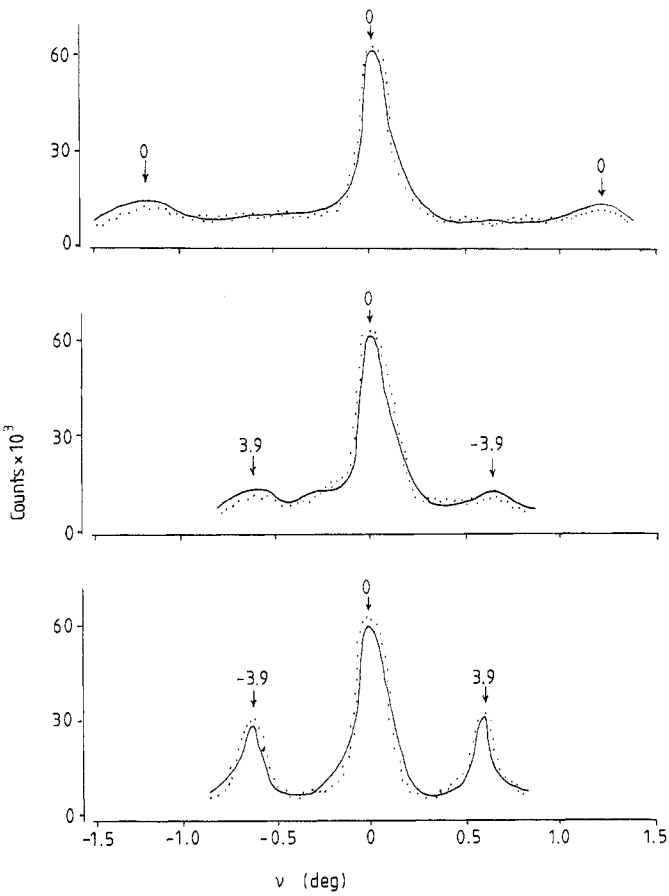

Figure 5. Observed and calculated profiles for $(003)_m$ and the satellites for $NiBr_2$ at 22 K. The full circles show observed data and the full curves were calculated. The arrows give values of ω (in deg).

Acknowledgments

We are grateful to Oxford University for providing the sample material, to the Institut Laue–Langevin, Grenoble, for providing neutron beam time on the multidetector four-circle diffractometer D16, and to the College of Engineering, University of Baghdad, for making computer facilities available to us.

Appendix 1. The geometry of the (003) reflection and satellite in reciprocal space

For the geometry, see figure A1. Note the following:

$$2\theta_{(003)} = 2A \sin [(\lambda/2)d^*_{(003)}] \qquad \omega = A \tan (\tau/d^*_{(003)})$$

$$2\theta_{sat} = 2A \sin [(\lambda/2)d^*_{sat}] \qquad \nu = \tau\lambda(180/\pi).$$

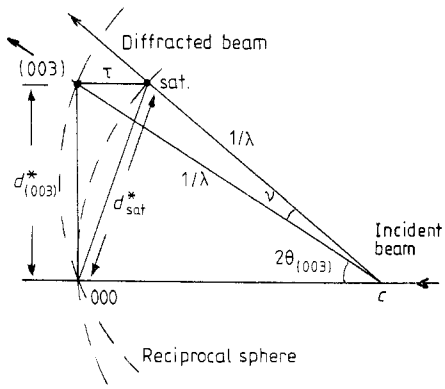

Figure A1

Appendix 2. The calculation of the elements 2θ, ω and ν

See figure A2, noting the following:

$$2\theta_{element} = D \tan 2\theta/(2.54\ \text{mm})$$

$$\omega_{element} = \omega°/(\text{step angle}) = \omega°/0.5°$$

$$\nu_{element} = D \tan \nu/(4.8\ \text{mm}).$$

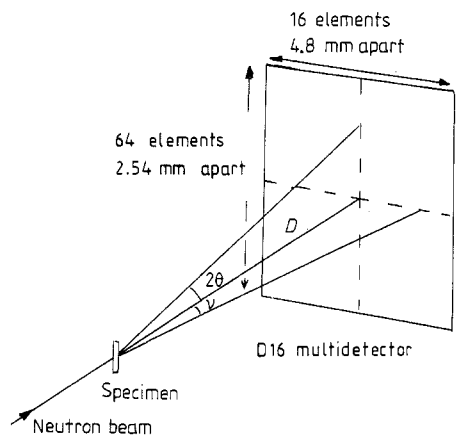

Figure A2

References

Adam A, Billerey D, Terrier C, Mainard R, Regnault L P, Rossat-Mignod J and Meriel P 1980 *Solid State Commun.* **35** 1
Day P, Dinsdale A, Krausz E R and Robbin D J 1976 *J. Phys. C: Solid State Phys.* **9** 2481
Day P, Moor M W, Wilkinson C and Ziebeck K R A 1981 *J. Phys. C: Solid State Phys.* **14** 3423
Day P and Ziebeck K R A 1979 *ILL Annual Report No* 147
—— 1980 *J. Phys. C: Solid State Phys.* **13** L523
Rastelli E, Tassi A and Reatto L 1979 *Physica* B **97** 1
Regnault L P, Rossat-Mignod, Adam A, Billerey D and Terrier C 1982 *J. Physique* **43** 1283